STUDIA UBB CHEMIA, LXI, 3, Tom I, 2016 (p. 285-294)
(RECOMMENDED CITATION)

Dedicated to Professor Luminița Silaghi-Dumitrescu on the Occasion of Her 65th Anniversary

THEORETICAL INVESTIGATION OF SYMMETRICAL THREE-TERMINAL JUNCTIONS

KATALIN NAGY[a], CSABA L. NAGY[a]*, MIRCEA V. DIUDEA[a]

ABSTRACT. In the present study atomistic models of three-terminal Y junctions with D_{3h} symmetry were built by the covalent assembly of single-walled armchair carbon nanotubes and the energetic properties were evaluated using quantum chemical methods at the PM6 level of theory. The theoretical study follows the influence of the relative position of the heptagonal ring defects on the structure and stability of the junction. The deformation of the attached nanotube branches is discussed in terms of the evaluated geometric parameters. Results indicate that the size of the junction and the diameter of the nanotube will determine the proper position of the defects corresponding to the energetically favourable cluster.

Keywords: *armchair carbon nanotubes, three-terminal junctions, PM6, POAV*

INTRODUCTION

Theoretical works predicted [1] and experimentally it was confirmed [2,3] that the electronic property of a single-walled carbon nanotube (SWCNT) strongly depends on the chiral vector – the direction along the graphene sheet is folded into the nanotube. Since carbon nanotubes can be both metals and semiconductors, this makes them promising candidates for miniaturizing electronics [4]. This would mean that silicon-based devices would be eventually replaced by all-carbon systems. The building blocks of such devices are the SWCNT junctions [5]. The unique electrical and mechanical properties of single nanotubes are reduced when they are joined electrostatically and share only a small contact area [6,7]. However the assembly of the quasi one-dimensional carbon nanotubes into an ordered covalent network remains a challenge in nanotechnology.

[a] *Babeş-Bolyai University, Faculty of Chemistry and Chemical Engineering, Arany Janos 11, RO-400028, Cluj-Napoca, Romania*
** Corresponding author: nc35@chem.ubbcluj.ro*

It is required that topological defects (non-hexagonal rings) to be introduced into the hexagonal lattice when assembling SWCNT junctions, so that the sp^2 electron configuration of each atom is retained. Experiments have demonstrated [8,9] that the creation of defects by damaging the material is necessary for nanotubes to be merged covalently. High-temperature electron beam irradiation [8] or the use of atomic welders [9] of crossing nanotubes during heat treatment have demonstrated to create the necessary instability to allow the joining of nanotubes. A recent review [7] summarizes all the progress and techniques made towards welding carbon nanotubes to obtain novel architectures. Related theoretical studies [10-15] have shown that pentagon-heptagon defects allow nanotubes to be joined in junctions with different morphology.

Soon after the discovery of multiwall carbon nanotubes the first symmetrical three-terminal SWCNT junction was theoretically proposed by Scuseria [16] and later they have been observed in electric arc experiments [17, 18]. Controlled growth of Y junctions has been achieved by template based synthesis using alumina with branching microchannels [19]. By the pyrolysis of methane over cobalt supported on magnesium oxide [20] Y junctions with straight branches and uniform diameters have been obtained, where the angles between the three arms are close to 120°.

'Super'-carbon nanostructures, including 'super' graphene-sheet [21] which is the rolled up to form 'super' single-walled nanotubes [21] and also topologically closed 'super'-fullerenes [22] have been proposed. Following the topology of a known carbon nanostructure the 'super' structures were constructed by replacing the sp^2 carbon atoms with Y-junctions and the carbon-carbon bonds with nanotubes resulting macromolecules with high-porosity. Their properties have been evaluated using tight-binding and density of states calculations and molecular dynamics simulations [21,22].

RESULTS AND DISCUSSION

The Y shaped nanotube junctions (Yj) studied in the present work are built by the covalent interconnection of three of the same finite length armchair single walled nanotubes which intersect each other at 120°, and are defined by (4,4), (6,6), (8,8) and (10,10) chiral vectors. The built structural models have D_{3h} symmetry and require six heptagonal rings as determined by the Euler polyhedral formula. The relative position of these defects located at the conjunction areas defines the morphology of the structure.

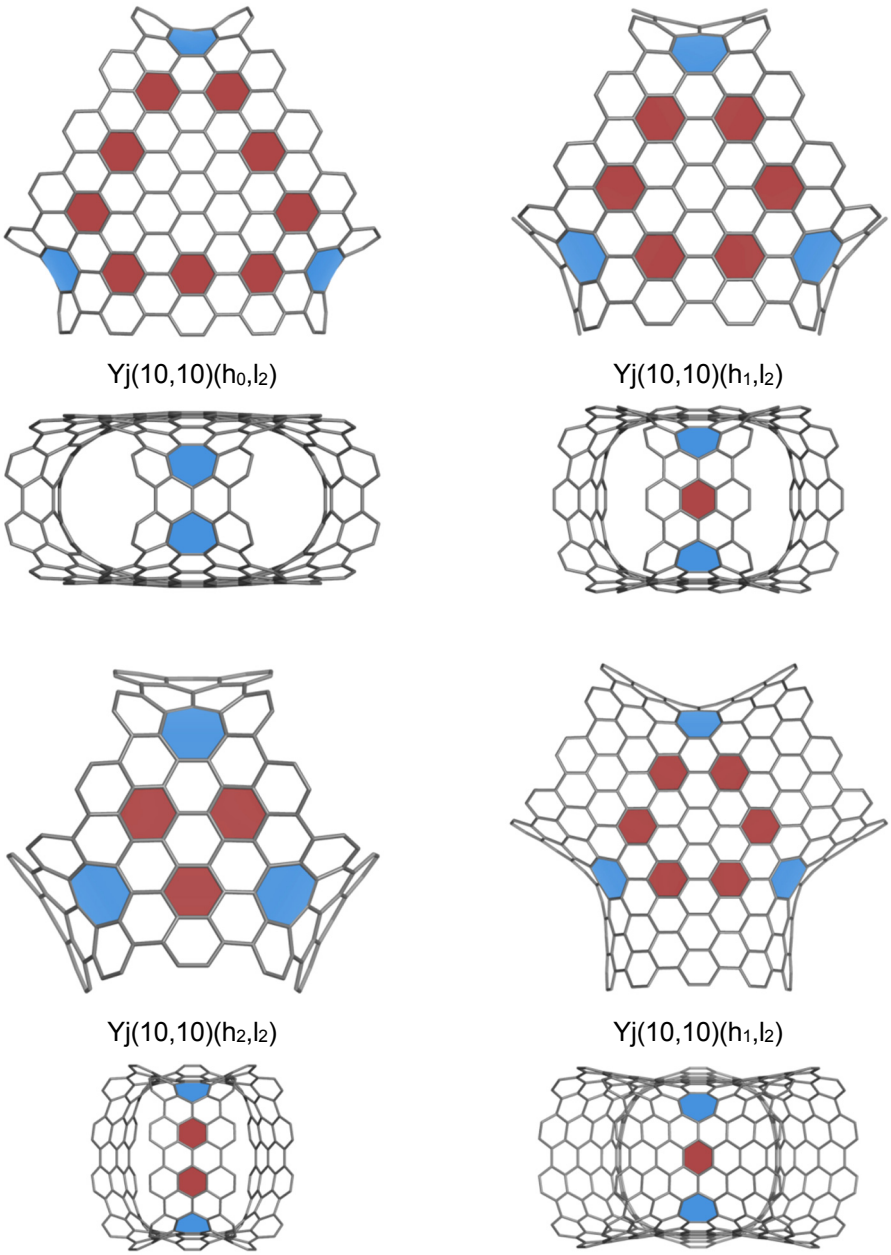

Figure 1. PM6 optimized geometries of the Yj(10,10) junctions viewed along the C_3 (top view) and C_2 axis (side view), respectively. Position of the heptagonal rings is highlighted in light blue, while the hexagons are shaded in dark red.

To the openings of the junction armchair carbon nanotubes are covalently attached (junction branches), resulting a seamless connection where all carbon atoms preserve the sp^2 hybridization state. Hydrogen atoms were used for saturating the dangling bonds located at the junction boundaries. From each Yj a short-branch and a long-branch junction were derived by attaching a nanotube of length 2 and 5.

To label the structures the nanotube chirality, the location of heptagons and the branch length is given. Here *h* refers to the number of hexagonal rings between the two heptagons as viewed from the side of the structure, whereas *l* defines the number of layers of carbon atoms in the junction branch and equals to the length of the nanotube. Notice that when *l*=2 for armchair nanotubes it corresponds to the nanotube unit cell.

The relative position of the six heptagonal rings not only defines the morphology and electronic properties of the junction, but also alters the shape of the attached nanotube from a circular to an elliptic cross section. Figure 1 presents the optimized geometries of the Yj(10,10) junctions viewed from the top and the side of the structures. Heptagonal rings are shaded in light blue, while to make it easier to follow the hexagons located between the sevenfold rings are highlighted in dark red. When *h* equals zero, two heptagons located at the side of the junction are at one bond length distance from each other (see example Yj(10,10)(h_0,l_2) in Figure 1). As *h* increases the number of hexagons decrease as viewed from the top of the molecule.

It can be observed in Figure 1 (side view) that in the case of structures Yj(10,10)(h_0,l_2) and Yj(10,10)(h_2,l_2) the cross section of the nanotube branches is elliptical. On the other hand junction Yj(10,10)(h_1,l_2) has a close circular cross section, which transforms to a better circular shape when the attached nanotube is longer, as it can be seen in case of Yj(10,10)(h_1,l_2). This concludes that the length of the nanotube will have an influence on the morphology of the junction, where longer nanotubes rather than changing the cross sectional shape will force the junction opening to have a close to circular outline.

Notice that in the case of the (8,8) and (10,10) nanotubes it is possible to build the Yj(8,8)(h_2,l_2) and Yj(10,10)(h_3,l_2) junctions, respectively. However, during geometry optimization the junction becomes highly distorted, therefore these structures have been excluded from the study. We presume that as the diameter of the nanotube increases, it is more likely that the energetically favoured junction will have the heptagons located closer to the side of the structure.

During energy minimization by employing the PM6 method the symmetry of the structure has been preserved. To verify if global minimum is reached, deformed initial geometries have been also used and no symmetry constraints have been used during geometry optimization.

Table 1. Binding energies (BE/N_C in kcal/mol), gap energies (E_{gap} in eV), and total energies (E_{tot} in kcal/mol) obtained at the PM6 level of theory.

	Label	Formula	BE/N_C (kcal/mol)	E_{gap} (eV)	E_{tot} (kcal/mol)
1	Yj(4,4)(h_0,l_2)	$C_{90}H_{24}$	220.988	5.865	764.212
2	Yj(4,4)(h_0,l_5)	$C_{162}H_{24}$	214.363	5.013	1448.482
3	Yj(6,6)(h_0,l_2)	$C_{150}H_{36}$	222.704	5.764	807.879
4	Yj(6,6)(h_0,l_5)	$C_{258}H_{36}$	217.491	5.007	1384.013
5	Yj(6,6)(h_1,l_2)	$C_{132}H_{36}$	223.446	*5.998*	838.068
6	Yj(6,6)(h_1,l_5)	$C_{240}H_{36}$	216.387	4.923	1683.232
7	Yj(8,8)(h_0,l_2)	$C_{222}H_{48}$	222.399	5.371	988.376
8	Yj(8,8)(h_0,l_5)	$C_{366}H_{48}$	218.063	4.747	1594.005
9	Yj(8,8)(h_1,l_2)	$C_{192}H_{48}$	223.751	5.844	933.147
10	Yj(8,8)(h_1,l_5)	$C_{336}H_{48}$	218.279	5.047	1595.893
11	Yj(10,10)(h_0,l_2)	$C_{306}H_{60}$	221.834	5.042	1214.064
12	Yj(10,10)(h_0,l_5)	$C_{486}H_{60}$	218.133	4.510	1888.225
13	Yj(10,10)(h_1,l_2)	$C_{264}H_{60}$	223.117	5.406	1137.863
14	Yj(10,10)(h_1,l_5)	$C_{444}H_{60}$	218.546	4.784	1811.677
15	Yj(10,10)(h_2,l_2)	$C_{234}H_{60}$	224.434	5.867	1055.472
16	Yj(10,10)(h_2,l_5)	$C_{414}H_{60}$	218.706	5.018	1834.199

To evaluate the stability of the structures the binding energy (BE/N_C in kcal/mol) divided by the number of carbon atoms and the gap energy (E_{gap} in eV) have been followed as a measure of thermodynamic and kinetic stability. The results for the 16 studied junctions obtained at the PM6 level of theory are listed in Table 1.

When the HOMO-LUMO gap energies of the short- and long-branch nanotube junctions are compared, it can be observed in each case that the shorter junction has the higher gap. This property of a vanishing gap with the length of the nanotube has been previously published [23].

Among the studied junctions Yj(6,6)(h_1,l_2) is the most kinetically stable with a gap value of ~6 eV. This is followed closely by structures 15, 1, and 9 with gap values of 5.867, 5.865, and 5.844, respectively. All these structures are short-branched Y-junctions. It can be observed that this stability order is not affected by the size of the structure (number of carbon atoms). In each series of junctions having the same chirality, the gap energy increases with the value of *h*. This fact indicates that the junction is the most relaxed when the heptagons are located at the corresponding position. This observation could be compared with the preferential position of pentagonal rings in case of fullerene isomers.

The binding energy per atom values (Table 1) do not give the same stability ordering as in the case of the gap energy. Higher binding energy values indicate a larger stability of the cluster. Structure 15 has the largest binding energy (224.434 kcal/mol), followed by junctions 9, 5, and 13 in decreasing order (223.751, 223.446, and 223.117 kcal/mol, respectively). Once again the energy values cannot be associated with the cluster size.

Table 2. Average piramidalization angles (θ_P) per carbon atom evaluated as defined by the POAV theory.

Label	Yj		Yj arm		Yj core	
	N_C	θ_P	N_C	θ_P	N_C	θ_P
Yj(4,4)(h_0,l_2)	90	4.107	48	4.119	42	4.093
Yj(4,4)(h_0,l_5)	162	5.755	120	6.117	42	4.719
Yj(6,6)(h_0,l_2)	150	2.490	72	2.755	78	2.246
Yj(6,6)(h_0,l_5)	258	3.550	180	3.934	78	2.662
Yj(6,6)(h_1,l_2)	132	2.502	72	2.663	60	2.308
Yj(6,6)(h_1,l_5)	240	3.910	180	3.898	60	3.947
Yj(8,8)(h_0,l_2)	222	1.707	96	1.994	126	1.489
Yj(8,8)(h_0,l_5)	366	2.477	240	2.814	126	1.834
Yj(8,8)(h_1,l_2)	192	1.528	96	1.964	96	1.091
Yj(8,8)(h_1,l_5)	336	2.555	240	2.797	96	1.951
Yj(10,10)(h_0,l_2)	306	1.271	120	1.564	186	1.081
Yj(10,10)(h_0,l_5)	486	1.888	300	2.157	186	1.454
Yj(10,10)(h_1,l_2)	264	1.071	120	1.492	144	0.720
Yj(10,10)(h_1,l_5)	444	1.917	300	2.119	144	1.495
Yj(10,10)(h_2,l_2)	234	1.274	120	1.544	114	0.990
Yj(10,10)(h_2,l_5)	414	1.841	300	2.158	114	1.008

To find a correlation between the energy of the Y junctions and the strain energy of the carbon atoms associated with the pyramidalization angles (θ_P), a POAV study was also performed. These values are presented in Table 2, and give a good estimate about the strain in the local geometry of carbon atoms. In Table 2 the average (per carbon atom) values are presented for the whole structure, and also for both the junction core and branches. The θ_P values of Yj arm can be compared with the one obtained for the single-walled nanotubes, and it is an indicator of the deformation from the perfect tubular shape. In case of armchair nanotubes (4,4), (6,6), (8,8) and (10,10) with five layers of carbon atoms the θ_P values are 4.187, 2.556, 1.786, and 1.355, respectively. It can be observed that in case of the junctions the attached nanotube is more strained having larger θ_P values.

The θ_P values listed for junctions Yj(10,10) can be easily compared with the optimized geometries from Figure 1. Notice that structure 13 has a less deformed attached nanotube than in the case of junctions 11 and 15. The junction core is also the most relaxed one in case of structure 13. The global θ_P value indicates that the least strained structure is Yj(10,10)(h_1,l_2), whereas the most strained short-branched junction is 1, which is in contrast with the gap value stability ordering.

To compare the local strain with the geometry of the structural fragments, the tubularity (T) of the nanotube branch, and the sphericity (S) of the junction core were computed. A quantitative measure of the attached nanotube tubularity defined by geometry can be expressed as:

$$T = \sqrt{\left(N_C \sum_{i=1}^{N_C} r_i^2 \right) \cdot \left(\sum_{i=1}^{N_C} r_i \right)^{-2}} - 1$$

where N_C represents the number of carbon atoms in one layer of the nanotube, whereas r_i is the distance of each carbon atom to the mass center of the given atom layer. It is based on finding the radius of a circle for each layer of carbon atoms, such that the sum of squares of the distance from each atom to this least-squares circle is minimal. In a similar way a measure of sphericity of the junction core can be defined [24].

In case of an armchair nanotube where all carbon atoms in a layer are arranged on a circle, the value of tubularity is zero. The larger the distortion of the nanotube the higher the values of T are.

Table 3 lists the sphericity and tubularity values obtained for the short-branched (10,10) Y-junctions. It can be observed that the shape of the tube cross-section is nearly circular in case of structure 13. Sphericity of the junction core increases with the decrease of the number of carbon atoms in the core section.

Table 3. Sphericity (S) of the junction core, tubularity (T) of the junction arm, the maximum (r_{max}), minimum (r_{min}), and average (r_{avg}) radius (in Å) of both structural fragments for Yj(10,10) short-branched junctions.

Label	Yj core				Yj arm			
	S	r_{avg}	r_{max}	r_{min}	T	r_{avg}	r_{max}	r_{min}
Yj(10,10)(h_0,l_2)	0.178	7.78	10.10	5.43	0.059	10.92	11.76	10.03
Yj(10,10)(h_1,l_2)	0.130	7.67	8.94	5.84	0.024	10.15	10.44	9.80
Yj(10,10)(h_2,l_2)	0.053	7.64	8.10	6.75	0.047	9.42	9.87	8.81

CONCLUSIONS

A set of 16 finite length single-walled armchair carbon nanotube Y junctions with D_{3h} symmetry has been investigated using quantum chemistry calculations employing the PM6 Hamiltonian. The present study adds valuable information about the influence on the structure and electronic properties of the relative position of the six heptagonal defects included at the conjunction of the nanotubes. Although the stability ordering by different parameters is not always pertinent, the obtained results indicate that structures are more relaxed if the non-hexagonal defects in case of Y junctions are located at the side of the structure. Shape of the junction core and the attached tubular branches are in good correlation with the structure stability as evaluated by various geometrical parameters.

COMPUTATIONAL DETAILS

The initial geometries have been fully optimized in the given symmetry using a tight SCF convergence criteria using the semiempirical parametrization method 6 (PM6) [25] as implemented in the Gaussian 09 program package [26]. The optimization of the open-ended structures has been carried out with the saturation of the dangling bonds with hydrogens, appearing at the outer layer of carbon atoms. Harmonic vibrational analysis confirms that they are local minima on the potential energy hypersurface.

On the optimized geometries the strain energy of the three-connected carbon atoms have been evaluated by computing the piramidalization angles (θ_P) according to the π-orbital axis vector (POAV) theory [27].

ACKNOWLEDGMENTS

The authors acknowledge the financial support offered by UEFISCDI under the project number PN-II-ID-PCE-2011-3-0346.

REFERENCES

1. R. Saito, M. Fujita, G. Dresselhaus, M.S. Dresselhaus, *Applied Physics Letters*, **1992**, *60*, 2204.
2. T.W. Odom, J.L. Huang, P. Kim, C.M. Lieber, *Nature*, **1998**, *391*, 62.

3. J.W. G. Wildöer, L.C. Venema, A.G. Rinzler, R.E. Smalley, C. Dekker, *Nature*, **1998**, *391*, 59.
4. L. Chico, V.H. Crespi, L.X. Benedict, S.G. Louie, M.L. Cohen, *Physical Review Letters*, **1996**, *76*, 971.
5. H.W.C. Postma, T. Teepen, Z. Yao, M. Grifoni, C. Dekker, *Science*, **2001**, *293*, 76.
6. J.M. Romo-Herrera, M. Terrones, H. Terrones, S. Dag, V. Meunier, *Nano Letters*, **2007**, *7*, 570.
7. G.S. Roberts, P. Singjai, *Nanoscale*, **2011**, *3*, 4503.
8. M. Terrones, F. Banhart, N. Grobert, J.C. Charlier, H. Terrones, P.M. Ajayan, *Physical Review Letters*, **2002**, *89*, 075505/1.
9. M. Endo, H. Muramatsu, T. Hayashi, Y.A. Kim, G. Van Lier, J.C. Charlier, H. Terrones, M. Terrones, M.S. Dresselhaus, *Nano Letters*, **2005**, *5*, 1099.
10. A.N. Andriotis, M. Menon, D. Srivastava, L. Chernozatonskii, *Physical Review Letters*, **2001**, *87*, 668021.
11. J.C. Charlier, T.W. Ebbesen, P. Lambin, *Physical Review B - Condensed Matter and Materials Physics*, **1996**, *53*, 11108.
12. B. Gan, J. Ahn, Q. Zhang, Q.F. Huang, C. Kerlit, S.F. Yoon, Rusli, V.A. Ligachev, X.B. Zhang, W. Z. Li, *Materials Letters*, **2000**, *45*, 315.
13. M. Menon, A.N. Andriotis, D. Srivastava, I. Ponomareva, L.A. Chernozatonskii, *Phys. Rev. Lett.*, **2003**, *91*, 4.
14. M. Menon, D. Srivastava, *Physical Review Letters*, **1997**, *79*, 4453.
15. R. Saito, G. Dresselhaus, M.S. Dresselhaus, *Physical Review B - Condensed Matter and Materials Physics*, **1996**, *53*, 2044.
16. G.E. Scuseria, *Chemical Physics Letters*, **1992**, *195*, 534.
17. L.A. Chernozatonskii, *Physics Letters A*, **1992**, *172*, 173.
18. D. Zhou, S. Seraphin, *Chemical Physics Letters*, **1995**, *238*, 286.
19. J. Li, C. Papadopoulos and J. Xu, *Nature*, **1999**, *402*, 253.
20. W.Z. Li, J.G. Wen and Z.F. Ren, *Applied Physics Letters*, **2001**, *79*, 1879.
21. V.R. Coluci, R.P.B. Dos Santos, D.S. Galvão, *Journal of Nanoscience and Nanotechnology*, **2010**, *10*, 4378.
22. V.R. Coluci, D.S. Galvao, A. Jorio, *Nanotechnology*, **2006**, *17*, 617.
23. K. Nagy, C.L. Nagy, “Hypergraphene from Armchair Nanotube Y Junctions”, in: M.V. Diudea, C.L. Nagy, (Eds.), “Diamond and Related Nanostructures”, Springer, Dordrecht, **2013**, chapter 11.
24. Y. Wang, M. Alcami, F. Martin, “Stability of Charged Fullerenes”, in: K.D. Sattler, (Ed.), “Handbook of Nanophysics: Clusters and Fullerenes”, CRC Press, Boca Raton, **2010**, chapter 25.
25. J.J.P. Stewart, *Journal of Molecular Modeling*, **2007**, *13*, 1173.

26. M.J. Frisch, G.W. Trucks, H.B. Schlegel, G.E. Scuseria, M.A. Robb, J.R. Cheeseman, G. Scalmani, V. Barone, B. Mennucci, G.A. Petersson, H. Nakatsuji, M. Caricato, X. Li, H.P. Hratchian, A.F. Izmaylov, J. Bloino, G. Zheng, J.L. Sonnenberg, M. Hada, M. Ehara, K. Toyota, R. Fukuda, J. Hasegawa, M. Ishida, T. Nakajima, Y. Honda, O. Kitao, H. Nakai, T. Vreven, J.A. Montgomery, Jr., J.E. Peralta, F. Ogliaro, M. Bearpark, J.J. Heyd, E. Brothers, K.N. Kudin, V.N. Staroverov, R. Kobayashi, J. Normand, K. Raghavachari, A. Rendell, J.C. Burant, S.S. Iyengar, J. Tomasi, M. Cossi, N. Rega, J.M. Millam, M. Klene, J.E. Knox, J.B. Cross, V. Bakken, C. Adamo, J. Jaramillo, R. Gomperts, R.E. Stratmann, O. Yazyev, A.J. Austin, R. Cammi, C. Pomelli, J.W. Ochterski, R.L. Martin, K. Morokuma, V.G. Zakrzewski, G.A. Voth, P. Salvador, J.J. Dannenberg, S. Dapprich, A.D. Daniels, Ö. Farkas, J.B. Foresman, J.V. Ortiz, J. Cioslowski, D.J. Fox, Gaussian 09, Revision A.02, Gaussian, Inc., Wallingford CT, 2009.
27. R.C. Haddon, K. Raghavachari, *Tetrahedron*, **1996**, *52*, 5207.